

Concise and high-fidelity predictive criteria for maximizing performance and robustness of bistable energy harvesters

R. L. Harné, M. Thota, and K. W. Wang

Citation: *Appl. Phys. Lett.* **102**, 053903 (2013); doi: 10.1063/1.4790381

View online: <http://dx.doi.org/10.1063/1.4790381>

View Table of Contents: <http://apl.aip.org/resource/1/APPLAB/v102/i5>

Published by the [American Institute of Physics](http://www.aip.org).

Related Articles

Random analysis on controlled buckling structure for energy harvesting
Appl. Phys. Lett. **102**, 041915 (2013)

Vibration energy harvesting using a phononic crystal with point defect states
Appl. Phys. Lett. **102**, 034103 (2013)

Phase transitions and thermal expansion in pyroelectric energy conversion
Appl. Phys. Lett. **102**, 023906 (2013)

Hybrid chromophore/template nanostructures: A customizable platform material for solar energy storage and conversion
J. Chem. Phys. **138**, 034303 (2013)

Bistable springs for wideband microelectromechanical energy harvesters
Appl. Phys. Lett. **102**, 023904 (2013)

Additional information on *Appl. Phys. Lett.*

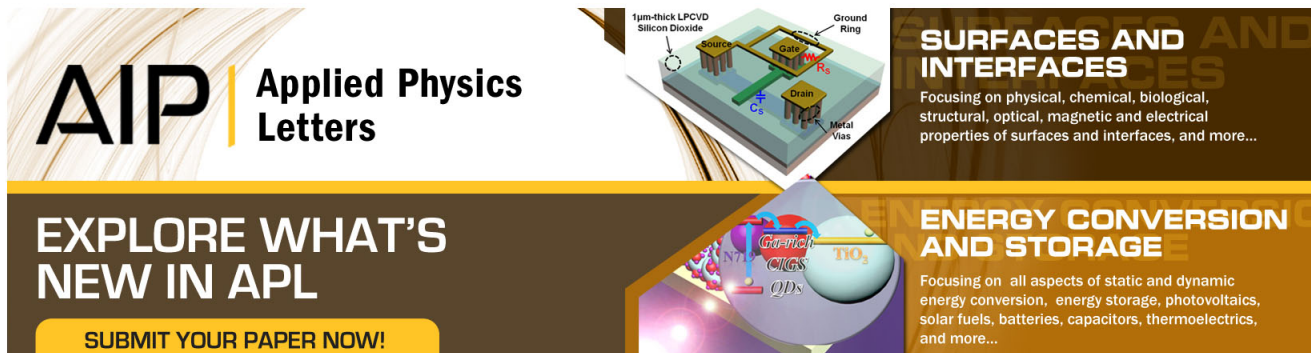
Journal Homepage: <http://apl.aip.org/>

Journal Information: http://apl.aip.org/about/about_the_journal

Top downloads: http://apl.aip.org/features/most_downloaded

Information for Authors: <http://apl.aip.org/authors>

ADVERTISEMENT



AIP | Applied Physics
Letters

SURFACES AND INTERFACES
Focusing on physical, chemical, biological, structural, optical, magnetic and electrical properties of surfaces and interfaces, and more...

ENERGY CONVERSION AND STORAGE
Focusing on all aspects of static and dynamic energy conversion, energy storage, photovoltaics, solar fuels, batteries, capacitors, thermoelectrics, and more...

EXPLORE WHAT'S NEW IN APL

SUBMIT YOUR PAPER NOW!

The advertisement features a central diagram of a microdevice with labels: 1µm-thick LPCVD Silicon Dioxide, Source, Drain, Metal Vias, Ground Ring, and a central gate structure. Below this, there is a diagram of energy conversion components including a QD (Quantum Dot), CIGS (Copper Indium Gallium Sulfide), and NO₂.

Concise and high-fidelity predictive criteria for maximizing performance and robustness of bistable energy harvesters

R. L. Harne,^{a)} M. Thota, and K. W. Wang

Department of Mechanical Engineering, University of Michigan, Ann Arbor, Michigan 48109, USA

(Received 24 September 2012; accepted 21 January 2013; published online 5 February 2013)

We employ an analytical model of a harmonically excited bistable vibration energy harvester to determine criteria governing continuous high-energy orbit (HEO) dynamics that maximize harvesting performance. Derivation of the criteria stems from previously unexplored dynamic relationships predicted by the model indicating critical conditions for HEO; experimental evidence of the phenomenon is provided as validation. The criteria are vastly more concise than existing HEO prediction methodology and can more accurately delineate HEO boundaries. This research addresses an essential need to create effective tools for high performance and robust bistable harvester design. © 2013 American Institute of Physics. [<http://dx.doi.org/10.1063/1.4790381>]

In recent years, vibrational energy harvesting research has rapidly grown and presents the potential for self-powered electronics^{1,2} or large scale power generation.³ The interest in exploiting nonlinearities in energy harvester design has developed with an aim to broaden the beneficial bandwidth of operation of individual devices.⁴ Impact,⁵ monostable duffing,⁶ and bistable oscillators^{7–10} have received a bulk of such attention.

Bistable devices are of particular interest since the high displacement snap through effect of switching from one stable state to the other can generate high power output. A bistable energy harvester can be highly excited by realistic ambient vibration forms and spectra, maximizing performance as compared to linear or monostable Duffing harvester designs.^{10–12} However, bistable harvesters require proper configuration of the double-well restoring potential so as to trigger and sustain interwell oscillations or high-energy orbit (HEO). An improper design may inhibit continuous snap through, leading to intrawell oscillations (low-energy orbit (LEO)), multi-harmonic or chaotic interwell vibration, none of which are as beneficial as HEO from an energy harvesting perspective since response amplitude is small or the energy diffuses away from the driving frequency.

Observations and analyses of sinusoidally forced bistable oscillators exhibiting intrawell, chaotic, and periodic interwell vibration are historically grounded^{13,14} with several criteria developed to predict the onset of well escape.^{14,15} Melnikov theory was recently revisited for the bistable energy harvester although the results are known to underpredict the true excitation level for which HEO are sustainable.¹⁶ While the prediction of chaotic or HEO dynamics has generated a number of works,^{14–16} there remains a critical need for an accurate and easily comprehensible metric by which to determine this transition and, therefore, appropriately design a bistable energy harvester for high and robust performance.

In this research, we utilize a fundamental mathematical principle corresponding to an observable but not previously

examined critical case of bistable oscillator dynamics to derive simple and intuitive expressions for the excitation amplitude-frequency relationship required to sustain HEO. Considering an inductive bistable energy harvester design where electromechanical influences are assumed to be accumulated within the damping terms,^{1,11} the governing equation for the device is expressed¹⁷

$$x'' + \gamma x' - x + \beta x^3 = p \cos \omega t, \quad (1)$$

where x is displacement defined from the central unstable equilibrium, γ is damping, β is nonlinearity, p is excitation level, ω is excitation frequency, and $(\cdot)'$ indicates differentiation with respect to dimensionless time t . Governing Eq. (1) allows for the existence of a number of phenomena: LEO, HEO, chaotic vibrations, and sub/superharmonics.^{7–10} Furthermore, these dynamics may exist within a narrow confine of excitation parameters. Thus, it is critical to understand the relationship between excitation conditions and design parameters to sustain HEO most beneficial for energy harvesting.

A 1-term harmonic balance solution may be employed to solve Eq. (1)

$$x(t) = k(t) + m(t) \sin \omega t + n(t) \cos \omega t, \quad (2)$$

where k allows for the possibility that the oscillator may vibrate in LEO. The solution is alternatively expressed $x(t) = k(t) + r(t) \cos(\omega t - \phi(t))$ where displacement amplitude is $r = \sqrt{m^2 + n^2}$ and phase is computed from $\tan \phi = m/n$. Substituting Eq. (2) into Eq. (1), assuming slow-varying coefficients, steady-state response, and neglecting higher order terms, two cubic characteristic polynomials for variable r^2 are determined depending on whether one is interested in LEO ($k \neq 0$) or HEO ($k = 0$).

$$\frac{225}{16} \beta^2 r^6 - \frac{15}{2} \beta (2 - \omega^2) r^4 + [(2 - \omega^2)^2 + (\gamma \omega)^2] r^2 - p^2 = 0, \quad (3)$$

$$\frac{9}{16} \beta^2 r^6 - \frac{3}{2} \beta (1 + \omega^2) r^4 + [(1 + \omega^2)^2 + (\gamma \omega)^2] r^2 - p^2 = 0, \quad (4)$$

^{a)} Author to whom correspondence should be addressed. Electronic mail: rharne@umich.edu.

Eqs. (3) and (4) represent the characteristic cubic polynomials for LEO and HEO vibration, respectively. Solving Eq. (3) or (4) yields three roots that represent the possible response amplitudes for a given set of system parameters $(\rho, \omega, \gamma, \beta)$. The individual coefficients (k, m, n) may then be back-calculated,^{17,18} stability checked via Floquet theory,¹⁸ and the oscillator phase lag with respect to the excitation computed.

To determine roots of Eqs. (3) and (4), we employ the generic notation of cubic polynomial with variable s in the form $as^3 + bs^2 + cs + d = 0$ where the coefficients are related to the coefficients of Eqs. (3) and (4) by observation. The cubic polynomial roots are¹⁹

$$s_1 = -b/(3a) - G/(3a) - (b^2 - 3ac)/(3aG), \quad (5)$$

$$s_2 = -b/(3a) + G(1 + i\sqrt{3})/(6a) - (1 - i\sqrt{3})(b^2 - 3ac)/(6aG), \quad (6)$$

$$s_3 = -b/(3a) + G(1 - i\sqrt{3})/(6a) - (1 + i\sqrt{3})(b^2 - 3ac)/(6aG), \quad (7)$$

where $G = [(H + 2b^3 - 9abc + 27a^2d)/2]^{1/3}$ and $H = [(2b^3 - 9abc + 27a^2d)^2 - 4(b^2 - 3ac)^3]^{1/2}$.

Figs. 1(a) and 1(b) show the response and phase, respectively, of a bistable energy harvester computed for parameters $(p, \gamma, \beta) = (0.16, 0.05, 1)$. Stable HEO and LEO are mathematically coexistent over a portion of the bandwidth considered although only one would be physically realizable at a time. The concern for maximizing bistable energy har-

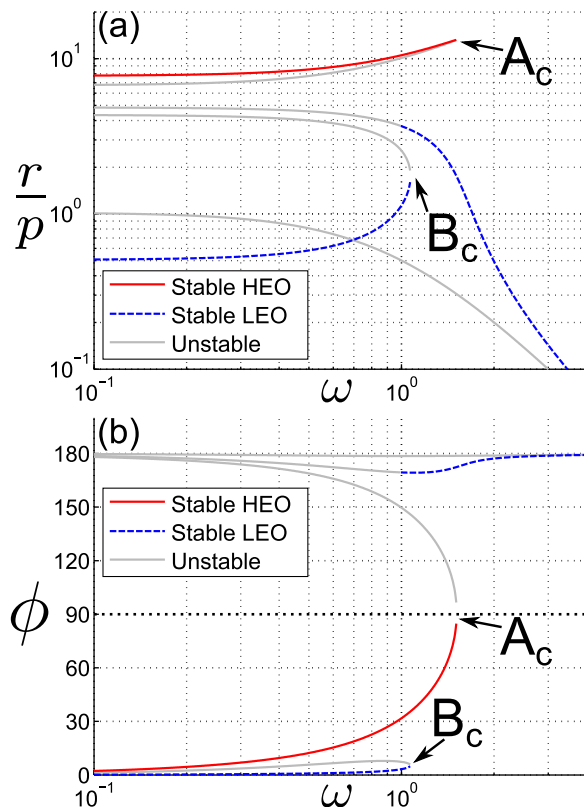


FIG. 1. Predicted bistable device (a) normalized response amplitude and (b) phase lag in degrees relative to excitation.

vester performance is to determine excitation parameters (p, ω) that truly provide for sustainable HEO vibration. The threshold conditions that demarcate HEO sustainability are presented by the points A_c and B_c in Fig. 1. Point A_c indicates the highest frequency HEO are possible while point B_c indicates a vertical tangency of LEO for which any increase in excitation level would induce HEO.¹⁵

Points A_c and B_c are also unique in Fig. 1 as the locations where two polynomial roots coalesce. This is plainly observed in the phase plot Fig. 1(b) since the unstable and stable branches merge and annihilate altogether. There are criteria for the coalescing of roots of cubic polynomials as well as a simple expression for the double root (here, a negative value for r^2 and thus an imaginary/non-physical response amplitude r). We aim to exploit the coalescing of roots to determine simple expressions for design requirements that demarcate HEO sustainability. Therefore, it becomes necessary to provide evidence that this mathematical feature is genuinely related to physical observation of a critical excitation level or frequency being passed. While point B_c shows a certain phase lag when coalescence occurs, it is seen that the specific phase lag changes as p varies, providing no repeatable feature to observe in experiments. However, it is found from any number of solutions of Eq. (4) that regardless of system parameters, point A_c always occurs with a phase lag of 90° . Despite the extensive research in bistable dynamics and energy harvesting,⁷⁻¹⁸ this unique feature does not appear to have been reported for bistable devices, although a similar phase relationship was observed for the peak resonance of monostable Duffing oscillators.²⁰ Thus, mathematical coalescing of roots in cubic polynomial Eq. (4) may be physically observed by a bistable oscillator in HEO vibration, which exhibits a phase lag of 90° immediately prior to losing HEO as a result of increasing ω beyond some critical value.

An experiment is conducted using a bistable oscillator, Fig. 2, having an inertial mass on a linear track with viscous damper and a bistable spring force attained by pre-compressing a spring at its upright position. The bistable device is attached to a shaker platform and the displacement

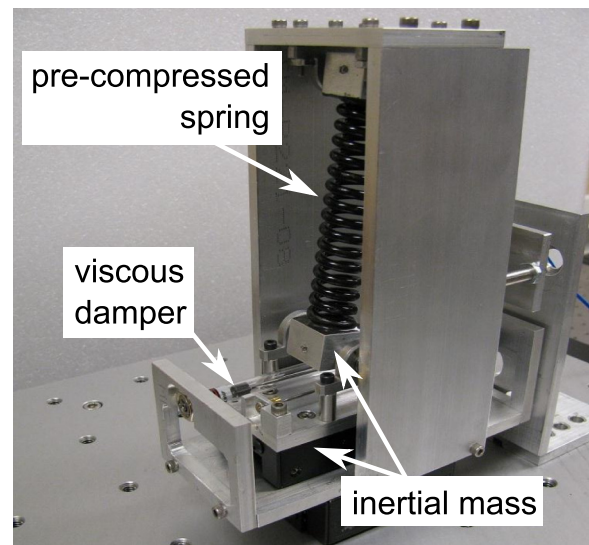


FIG. 2. Experimental bistable oscillator.

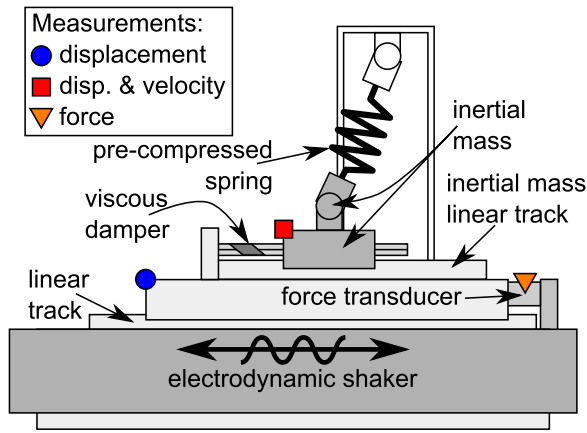


FIG. 3. Schematic of experimental setup.

and velocity of the inertial mass are measured using a laser vibrometer. The sinusoidal displacement and input force of the shaker table are measured using potentiometer and force transducer, respectively, the latter positioned between the shaker attachment and bistable device itself, Fig. 3. The device response amplitude and phase lag measured for constant excitation amplitude but varying frequency are presented in Figs. 4(a) and 4(b), respectively. Identically to point A_c in Fig. 1(b), the experimental results Fig. 4(b) show a phase lag approaching 90° prior to the bistable device losing HEO. This verifies that mathematical root-coalescence is indicative of realistic HEO sustainability boundaries. Furthermore, while Fig. 1(a) suggested that HEO are possible at all frequencies below a critical point, we observe in Fig. 4(a) that HEO are attainable only over specific bandwidth, as is commonly known.⁷⁻¹⁰ This feature justifies the importance for determining critical excitation parameters that lead to HEO as discussed in the following paragraphs, since the results in Fig. 1(a) are ambiguous in this matter.

Having verified that root coalescence for cubic polynomials is analogous to critical excitation values that define HEO sustainability, we aim to exploit the two cubic polynomials Eqs. (3) and (4) to determine criteria that serve as lower and higher bounds on the critical excitation amplitude-frequency ($p - \omega$) curve. When two roots coalesce into one, the following criterion is satisfied:

$$[(2b^3 - 9abc + 27a^2d)^2 - 4(b^2 - 3ac)^3]^{1/2} = 0. \quad (8)$$

We employ the cubic polynomial for HEO Eq. (4), substitute coefficients (a, b, c, d), and solve for the excitation amplitude. The resulting Eq. (9), criterion A, defines the critical excitation level p above which HEO will be sustainable for given (ω, γ, β).

$$p^2 = \frac{8}{81} \frac{1}{\beta} \{ (1 + \omega^2)[(1 + \omega^2)^2 + (3\gamma\omega)^2] - [(1 + \omega^2)^2 - 3(\gamma\omega)^2]^{3/2} \}. \quad (9)$$

To determine a lower bound for HEO attainment from the LEO cubic polynomial Eq. (3), we implement the double root expression itself, $s_d = (bc - 9ad)/[2(3ac - b^2)]$. It is found that the denominator is always negative for $\omega < 1$ for

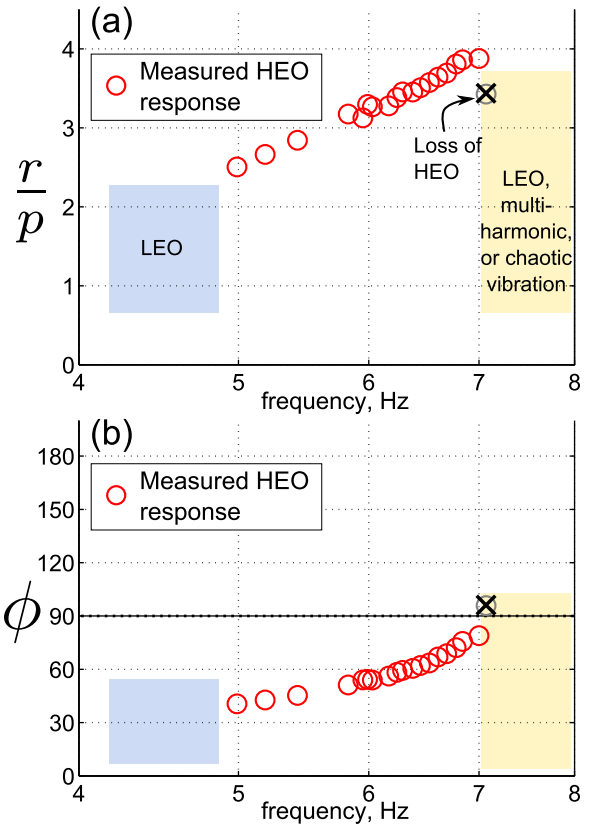


FIG. 4. Measured bistable device (a) normalized response amplitude and (b) phase lag in degrees relative to excitation.

most realistic oscillator damping, $\gamma < 0.75$. Should the numerator become positive, $bc - 9ad > 0$, then the double root r^2 is negative indicating that the response amplitude r is imaginary/non-physical, which characterizes the annihilation of roots in Fig. 1(a): in other words, LEO have been escaped into HEO. To find the critical condition, we set the numerator of s_d to zero, substitute coefficients (a, b, c, d) from Eq. (3), and solve for excitation amplitude. Eq. (10), criterion B, represents the excitation level which, when exceeded, will send the oscillator from LEO to HEO.

$$p^2 = \frac{1}{18} \frac{1}{\beta} (2 - \omega^2)[(2 - \omega^2)^2 + (\gamma\omega)^2]. \quad (10)$$

Eqs. (9) and (10) set boundaries for excitation level p for which HEO are sustainable. The derivations of criteria A and B have followed the insight provided by phenomenological root-coalescence observed as a characteristic phase relationship in experimentation indicating the roots of the cubic polynomials Eqs. (3) and (4) are reduced to a double root and real root. Past attempts to determine similar criteria have led to measures of varying accuracy and rarely to straightforward equations¹⁵ as compared with Eqs. (9) and (10). Melnikov theory provides the most tractable expression elsewhere in literature and was recently used in the study of the bistable energy harvester.¹⁶ The Melnikov criterion is²¹ $p = [\gamma\sqrt{2} \cosh(\omega\pi/2)]/[3\sqrt{\beta}(\omega\pi/2)]$. Melnikov predictions are known to be conservative in terms of achieving well escape,^{15,16} suggesting it could underestimate the excitation level required to sustain HEO.

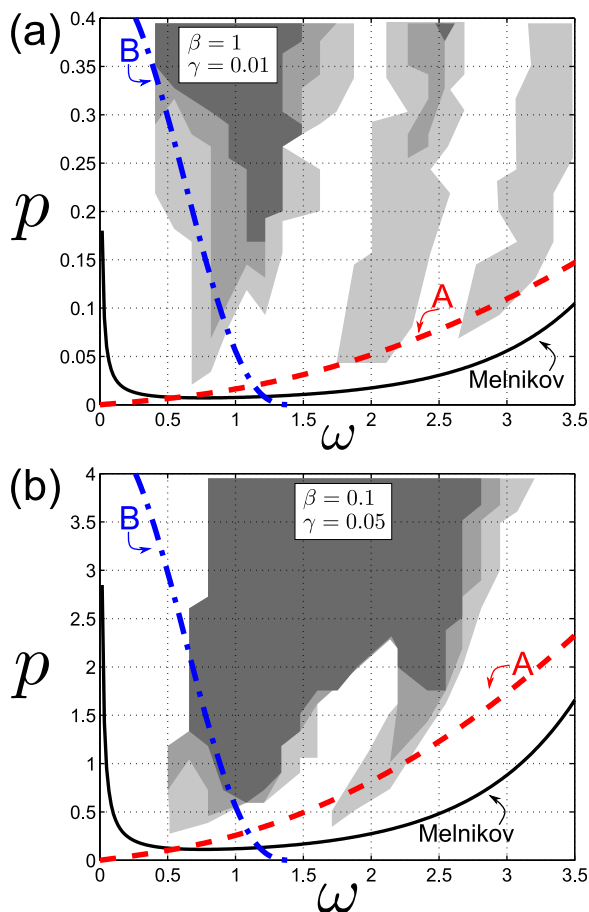


FIG. 5. Comparison of critical excitation amplitude-frequency curves for (a) $(\gamma, \beta) = (0.01, 1)$ and (b) $(\gamma, \beta) = (0.05, 0.1)$. Numerical simulation of HEO sustainability 10%, 50%, and 90% regions denoted by light, medium, and dark gray shading, respectively.

To test criteria A and B, we plot the results for two cases of system parameters in Fig. 5, for (a) $(\gamma, \beta) = (0.01, 1)$ and (b) $(\gamma, \beta) = (0.05, 0.1)$. Included in Fig. 5 are Melnikov predictions and results of numerically integrating governing Eq. (1) 50 times for each (p, ω) with unique initial conditions for every long-time evaluation. Simulations were conducted on a $p - \omega$ grid and Fig. 5 indicates regions where HEO (not multi-harmonic) was maintained for 10%, 50%, and 90% of the 50 simulations by light, medium, and dark gray shading, respectively.

From Fig. 5, it is clear that criteria A and B more closely bound the genuine cases of HEO sustainability where maximum harvesting performance is achieved, as compared to Melnikov predictions. Unshaded regions below A and B led

primarily to LEO while such areas above both A and B often yielded multiharmonic or chaotic response. Fig. 5 shows that criteria A and B lead to better predictions of HEO for two contrasting examples of damping and nonlinearity. Since the primary consequence of energy harvesting is a damping influence on the mechanical system,^{1,11} the results of Fig. 5(b) (high damping) are more representative of a realistic bistable harvester. The improved predictive capability of criteria A and B indicates they are substantially more effective as design tools.

In conclusion, this research addresses a critical need in creating effective tools for bistable harvester design. Maximizing the harvester performance and robustness by proper design in accordance to anticipated excitation characteristics necessitates accurate and comprehensible criteria to demarcate sustainable HEO. In this research, we derived criteria for HEO boundaries utilizing a dynamic phase phenomenon unexamined in previous studies and the corresponding mathematical principles. As compared with existing methods for HEO prediction, the proposed criteria offer significant improvements in terms of fidelity and conciseness.

¹C. B. Williams and R. B. Yates, *Sens. Actuators, A* **52**, 8 (1996).

²M. A. Karami and D. J. Inman, *Appl. Phys. Lett.* **100**, 042901 (2012).

³I. L. Cassidy, J. T. Scruggs, S. Behrens, and H. P. Gavin, *J. Intell. Mater. Syst. Struct.* **22**, 2009 (2011).

⁴L. Tang, Y. Yang, and C. K. Soh, *J. Intell. Mater. Syst. Struct.* **21**, 1867 (2010).

⁵L. Gu and C. Livermore, *Smart Mater. Struct.* **20**, 045004 (2011).

⁶B. P. Mann and N. D. Sims, *J. Sound Vib.* **319**, 515 (2009).

⁷A. F. Arrieta, P. Hagedorn, A. Erturk, and D. J. Inman, *Appl. Phys. Lett.* **97**, 104102 (2010).

⁸A. Erturk and D. J. Inman, *J. Sound Vib.* **330**, 2339 (2011).

⁹L. Tang, Y. Yang, and C.-K. Soh, *J. Intell. Mater. Syst. Struct.* **23**, 1433 (2012).

¹⁰R. L. Harne and K. W. Wang, *Smart Mater. Struct.* **22**, 023001 (2013).

¹¹M. F. Daqaq, *J. Sound Vib.* **330**, 2554 (2011).

¹²N. A. Khovanova and I. A. Khovanov, *Appl. Phys. Lett.* **99**, 144101 (2011).

¹³W.-Y. Tseng and J. Dugundji, *J. Appl. Mech.* **38**, 467 (1971).

¹⁴P. Holmes, *Philos. Trans. R. Soc. London, Ser. A* **292**, 419 (1979).

¹⁵W. Szemplińska-Stupnicka, *Nonlinear Dyn.* **7**, 129 (1995).

¹⁶S. C. Stanton, B. P. Mann, and B. A. M. Owens, *Physica D* **241**, 711 (2012).

¹⁷B. P. Mann, D. A. W. Barton, and B. A. M. Owens, *J. Intell. Mater. Syst. Struct.* **23**, 1451 (2012).

¹⁸S. C. Stanton, B. A. M. Owens, and B. P. Mann, *J. Sound Vib.* **331**, 3617 (2012).

¹⁹R. S. Burington, *Handbook of Mathematical Tables and Formulas* (McGraw-Hill, New York, 1973).

²⁰W. Szemplińska-Stupnicka, *Int. J. Nonlinear Mech.* **3**, 17 (1968).

²¹*The Duffing Equation: Nonlinear Oscillators and their Behaviour*, edited by I. Kovacic and M. J. Brennan (Wiley, Chichester, 2011).